LONG-TIME STATES OF INVERSE CASCADES IN THE PRESENCE OF A MAXIMUM LENGTH SCALE

by

Murshed Hossain, William H. Matthaeus, and David Montgomery

Physics Department

College of William and Mary

Williamsburg, Virginia 23185 USA

Abstract

It is shown numerically, both for the two-dimensional Navier-Stokes (guiding-center plasma) equations and for two-dimensional magnetohydrodynamics, that the long-time asymptotic state in a forced inverse-cascade situation is one in which the spectrum is completely dominated by its own fundamental. The growth continues until the fundamental is dissipatively limited by its own dissipation rate.

1. Introduction

It is by now well known that there exist circumstances under which the equations of some nonlinear continuous media exhibit turbulent solutions which transfer a global quantity to long wavelengths at a rate comparable to that at which the quantity is supplied. This is a reversal, for that quantity, of the older Kolmogoroff-Richardson picture of spectral transfer to short wavelengths and dissipation there. The first historically important case was the case of two-dimensional Navier-Stokes (2D NS) turbulence as initiated by Onsager (1949), Fjørtoft (1952), Kraichnan (1967), Batchelor (1969), Leith (1968), and Lilly (1969). The relevance of these calculations for plasma physics follows from the fact that the mathematics of the 2D NS case is identical to that of the electrostatic guiding-center plasma (e.g., Montgomery 1975).

The demonstration of similar long-wavelength transfer in three-dimensional, incompressible magnetohydrodynamics (3D MHD) was due to Frisch and collaborators (Frisch et al 1975 Pouquet et al 1976, Meneguzzi et al 1981). It was soon demonstrated that still a third quantity could be inversely transferred to long wavelengths in two-dimensional, incompressible magnetohydrodynamics (2D MHD) by Fyfe et al (1976, 1977a,b) and Pouquet (1978). A review of the literature up to 1980 appears in Kraichnan and Montgomery (1980).

Because of the difficulty of doing two-dimensional experiments, the cited work has all been theoretical and/or computational. The emphasis has been on power-law behavior for wavenumber spectra, following the influential conjecture of Kraichnan (1967) concerning two possible inertial subranges transferring energy and enstrophy in opposite directions. Some investigations of dissipation scale behavior have also been reported for the 2D MHD case (Orszag and Tang 1979, Matthaeus and Montgomery, 1980, 1981, Matthaeus 1982, Frisch et al, 1983).

Power laws are only obtained persuasively from dimensional analysis. In order for them to be seen clearly, they are thought to require very large Reynolds numbers (mechanical and/or magnetic) in order that the inertial subranges be cleanly separated from each other and from the dissipation range. High spatial resolution is required at these large Reynolds numbers, and it is accurate to say that no reported numerical solution has contained a wide enough range of wavenumbers to satisfy the chain of inequalities required for a satisfactory test of the power-law behavior in any putatively inverse-cascading situation. There is no question, however, that the qualitative effect of large back-transfer, at least not inconsistent with the proposed power laws, has been seen in numerical solutions of the relevant dynamical equations in all three cases (Lilly 1969, Fyfe et al 1977b, Meneguzzi et al 1981).

Theoretical predictions typically have been for unbounded systems, so that there were arbitrarily many additional octaves in wavelength for the spectrum of the injected and inversely-cascaded quantity to expand into at the lower end. Numerical solutions, however, always take place on periodic or finite grids, and thereby have associated with them a maximum wavelength (minimum wavenumber) beyond which the inversely-cascaded spectrum cannot go. Because of the slow time scales involved in the long-wavelength eddy turnover times and because of limited computer budgets, computations have not been reported for times long compared to the time required for the longest allowed wavelength to fill up. Both theory and computation have remained vague on the question of what happens in an inversely-cascading situation.

Here, we address this question numerically for both the 2D NS and 2D MHD cases. In both cases, the fields are driven by a prescribed random function, band-limited in wavenumber space, which serves as the source of the

excitations that are transferred elsewhere in the k space. The resolution of the computation is not high and the Reynolds numbers are not large. There is no pretense that the inertial subranges are well separated or that power-law predictions are verifiable. It is not necessary, however, to be in this high Reynolds number regime in order to see large amounts of back transfer, or to address the question of what happens to the back-transferred excitations when they have no lower place in wavenumber space to which to migrate. It is toward this latter, qualitative question that the following material is directed.

There would seem to be at least three possible scenarios for what might occur after the k spectrum fills in between the foreing band and the fundamental lowest wavenumber k_{min}. (1) The inverse spectral transfer might cease. (2) The relevant parts of the k spectrum might all rise together, possibly maintaining a power law behavior, with perhaps a "healing region" just below the foreing band. (3) The fundamental k_{min} might continue to absorb the supplied excitations, running off and leaving the rest of the spectrum, until it is limited by its own dissipation rate. These three may not exhaust the possibilities, but what we wish to demonstrate in the following pages is that alternative (3) is in fact what occurs, both for the 2D NS and 2D MHD cases. We are unaware of any previous predictions or tests of this effect.

In section 2, we outline the computational procedure by which the tests are carried out. In sections 3 and 4, respectively, results are reported for the 2D NS and 2D MHD cases. Section 5 describes some semi-quantitative attempts at modelling algebraically the k_{min}-dominated final state, and briefly summarizes our results. Questions of accuracy of the numerical method are addressed in the Appendix.

2. Numerical Procedure

The 2D MHD equations can be written in a standard dimensionless form which, by the omission of several terms, reduces to the 2D NS case. Specifically,

$$\frac{\partial \omega}{\partial t} = -\underset{\sim}{v}\cdot\nabla\omega + \underset{\sim}{B}\cdot\nabla J + \nu\nabla^2\omega + F \qquad (1)$$

$$\frac{\partial a}{\partial t} = -\underset{\sim}{v}\cdot\nabla a + \mu\nabla^2 a + G \qquad (2)$$

(see, e.g., Fyfe et al, 1976, 1977a,b). All fields are functions of x,y and the time t, and are independent of the z-coordinate. The vorticity is $\omega = -\nabla^2\psi$, where ψ is the stream function and the velocity $\underset{\sim}{v} = \nabla\psi\times\hat{e}_z$. The magnetic vector potential is $a\hat{e}_z$ and the magnetic field is $\underset{\sim}{B} = \nabla a\times\hat{e}_z$. The electric current density has only a z component and is $J = -\nabla^2 a$. The vector fields have only x and y components, $\underset{\sim}{v} = (v_x, v_y, 0)$ and $\underset{\sim}{B} = (B_x, B_y, 0)$, though a constant dc magnetic field $\underset{\sim}{B}_o = B_o\hat{e}_z$ can be added to $\underset{\sim}{B}$ without altering equations (1) and (2). Deleting equation (2) and setting $\underset{\sim}{B} = 0$ leaves the 2D NS system.

F and G are random forcing functions of x, y and t whose statistics will be described below.

Rectangular periodic boundary conditions are assumed, for all fields, over a square box of edge 2π. All fields are expressed as Fourier series with wavenumbers $\underset{\sim}{k} = (k_x, k_y)$ with integer components. For example, for the vorticity, $\omega = \Sigma_{\underset{\sim}{k}}\omega(\underset{\sim}{k},t)\exp(i\underset{\sim}{k}\cdot\underset{\sim}{x})$. Finite computational resourses make it necessary to truncate the Fourier series at the relatively low value of $|\underset{\sim}{k}|_{max} = k_{max} = 16$, though some runs with $k_{max} = 32$ have also been carried out. The mechanical and magnetic Reynolds numbers, ν^{-1} and μ^{-1}, must be chosen small enough to suppress wavenumbers significantly above k_{max}, for the results to be physical. The ν, μ chosen for the runs reported were never smaller than 0.002.

Solution of equations (1) and (2) is by the by-now standard Orszag-Patterson spectral method (Orszag 1971, Patterson and Orszag 1971, Gottlieb and Orszag 1977), which has proved extraordinarily useful in turbulence computations. As a time-stepping scheme, we use

$$Q^{n+1/2}(\underset{\sim}{k}) = Q^n(\underset{\sim}{k}) + P(Q^n(\underset{\sim}{k}))\Delta t/2, \tag{3}$$

$$Q^{n+1}(\underset{\sim}{k}) = Q^n(\underset{\sim}{k}) + P(Q^{n+1/2}(\underset{\sim}{k}))\Delta t. \tag{4}$$

Here $dQ(\underset{\sim}{k},t)/dt = P(Q(\underset{\sim}{k},t))$ stands symbolically for the Fourier-transformed version of either equation (1) or (2), and $Q(\underset{\sim}{k},t)$ represents all the Fourier coefficients of all the fields. The index n indexes the nth time step of duration Δt.

The forcing functions F and G have Fourier transforms $F(\underset{\sim}{k},t)$, $G(\underset{\sim}{k},t)$ which are chosen at each lattice point of the $\underset{\sim}{k}$ space, according to the following recipe. Let $H^n(\underset{\sim}{k})$ be the real or imaginary part of either $F(\underset{\sim}{k})$ or $G(\underset{\sim}{k})$ at time step n. Then (Fyfe et al, 1977b),

$$H^{n+1}(\underset{\sim}{k}) = f H^n(\underset{\sim}{k}) + \sqrt{1-f^2}\, J^n(\underset{\sim}{k}). \tag{5}$$

$J^n(\underset{\sim}{k})$ is a random number taken from a Gaussian random number generator. The "memory fraction" f is chosen between 0 and 1, and for the runs reported, we used f = 0.95 for both the 2D NS and 2D MHD runs. $F(\underset{\sim}{k},t)$ and $G(\underset{\sim}{k},t)$ are set identically zero outside a "forcing band" in wavenumber space, $k^2_{F_{min}} \le k^2 \le k^2_{F_{max}}$. In the runs reported, $k^2_{F_{min}} = 55$ and $k^2_{F_{max}} = 70$.

In both the 2D NS and 2D MHD runs, we started with an empty spectrum and followed the evolution over a considerably longer interval than previously (Fyfe 1977b). For the 2D MHD run, the F and G functions were uncorrelated, but acted in the same band between $k^2 = 55$ and 70, with statistically equal

magnitudes. The "filling up" of the spectrum at the longest wavelengths is a slow process, and consumes much computer time; it is an inherent feature of such computations, and is apparently the reason these computations have not been carried out previously.

3. 2D NS Case; Inverse Energy Cascade

Results for the Navier-Stokes run are shown in figures 1-6.

Figure 1 shows the total energy $E(t) = \sum_{\underset{\sim}{k}} E(\underset{\sim}{k}) = \frac{1}{2}\Sigma_{\underset{\sim}{k}} |\underset{\sim}{y}(\underset{\sim}{k},t)|^2$ as a function of time. The two most significant features of the curve are: (i) the total energy increases systematically with time, as is expected for an inversely cascading quantity; (ii) the total energy appears to be approaching asymptotically to a constant value, whereas for an unbounded system in the limit of infinite Reynolds numbers, a linear increase of $E(t)$ with t might be expected. As will be discussed in section 5, the curve in figure 1 is rather well fit by the expression $E = E_{max}[1-\exp(-t/\tau)]$ with $E_{max} = 3.9$ and $\tau = 124$.

Also in figure 1, we show, as squares, the energy contained in the fundamental $k^2 = k^2_{min} = 1$. It will be apparent that by $t \cong 30$, it already accounts for a significant fraction of the total.

Figure 2 shows the total enstrophy $\Omega = \sum_{\underset{\sim}{k}} \Omega(\underset{\sim}{k}) = \frac{1}{2}\Sigma_{\underset{\sim}{k}} |\omega(\underset{\sim}{k},t)|^2$ versus time. The enstrophy should be the directly cascading quantity, and reaches a value about which it fluctuates while the energy continues to grow.

Figures 3a and 3b show time averaged modal energy spectra $|\underset{\sim}{y}(\underset{\sim}{k})|^2$ versus k^2. These are averaged over all the values of $\underset{\sim}{k}$ corresponding to a given k^2. Figure 3a shows averages over 1000 time steps ending at $t = 29.3$, and figure 3b shows averages over 1000 time steps ending at $t = 273.44$. (Every fourth point is plotted for $k^2 \geq 70$, to avoid cluttering the graphs.)

The crucial result of this paper is thought to be illustrated by the fact that the fundamental has come to contain about ninety per cent of the total energy.

Though the separation of the spatial scales is far too scant to identify inertial subranges, we show in figures 3a,b least-squares, straight-line fits to the spectra above and below the forcing bands. In figure 3b, the exponents above and below are -1.16 and -1.62, corresponding to -1.32 and -2.24 for omnidirectional spectra, whereas the Kolmogoroff-style dimensional-analysis predictions are -1.67 and -3.0, omni-directional. We attach no particular importance to these numbers; the power-law predictions are inapplicable.

Figure 4 displays large-scale stream function contours of constant ψ at t = 273.44, showing the results of domination of the spectrum by the fundamental.

Figure 5 illustrates the behavior of a typical intermediate ($k^2 = 50$) modal energy, fluctuating about a nearly constant value. This should be contrasted with the continued growth of the fundamental displayed in figure 1.

Figure 6 exhibits the Carnevale (1981) entropy, $S \equiv \sum_{\underset{\sim}{k}} \ell n |\underset{\sim}{v}(\underset{\sim}{k},t)|^2$, as a function of time. The function quickly maximizes, and then gradually decays. The interpretation of the decay might loosely be that as the system becomes dominated by the fundamental, the effective degree of randomness decreases. (The action of viscosity is typically to <u>decrease</u> entropy.) This entropy has its origins in information theory, and descends from the Burg entropy (Burg, 1975).

4. <u>The MHD Case</u>

The results of the 2D MHD run are shown in figures 7-11. The spectrum is forced both mechanically and magnetically, with the ratio between F and G chosen to supply kinetic and magnetic energies at statistically equal rates.

The forcing band ($55 \leq k^2 \leq 70$) was chosen to be the same as in the Navier-Stokes case, and for the run we exhibit, $\mu = \nu = 0.01$, with a time step $t = 1/256$. MHD runs are typically noisier than NS ones, and the computed Kolmogoroff dissipation wave numbers tend to be higher. The $(32)^2$ runs we have performed with the above parameters tend to lead to Kolmogoroff dissipation wave numbers significantly greater than k_{max}. Even though the behavior exhibited for the 2D MHD case closely parallels the 2D NS behavior, for $(32)^2$, we have wought to enhance our confidence in the reality of the effect by also performing some $(64)^2$ runs. Because $(64)^2$ runs for times as long as those reported in section 3 are prohibitively expensive and time consuming, we have resorted to the following trick. We computed a $(32)^2$ run, starting with an empty spectrum, up to time 97,66. At this time, we used the computed Fourier coefficients as <u>initial</u> data for a 5000 time step run (up to $t = 117.19$) with a $(64)^2$ resolution. (Both the $(32)^2$ and $(64)^2$ runs were performed on a Cyber 203: a 64-bit machine that is essentially without round-off error.) Even though the Kolmogoroff dissipation wave number was unresolved by $k_{max}/k_{min} = 16$ during the first interval (typically, the dissipation wave number was 33), it was reasonably well resolved during the second interval (typically, the dissipation wave number was also about 33) when k_{max}/k_{min} was 32. No significant changes were observed from one piece of the run to the other; the second piece, regarded as accurate, continued the behavior observed in the first piece, regarded as possibly inaccurate.

Figure 7 shows the mean square vector potential vs. time, with squares illustrating the contribution of the fundamental $k^2_{min} = 1$ (again, values shown are averages over all values of $\underset{\sim}{k}$ corresponding to a given k^2).

The transition from a $(32)^2$ computation to a $(64)^2$ computation occurs at $t = 97.66$. Figure 8 shows, for the same run, the total energy vs. time; the points labeled "B" are the magnetic contributions, and the points labeled "V" are the mechanical (kinetic) energy. The higher values of magnetic energy are typical of forced MHD runs. Figures 7 and 8 should be compared with figures 1 and 2 for the Navier-Stokes case.

The vector potential spectrum ($|A(\underset{\sim}{k})|^2 = |\underset{\sim}{B}(\underset{\sim}{k})|^2/k^2$ vs. k^2) is shown in figure 9, averaged over 50 values, spaced 100 time steps apart, ending at $t = 97.66$. Figure 10 shows the vector potential spectrum, averaged over 25 values, spaced 100 time steps apart, ending at 117.19. The dominance of the spectrum by the fundamental should be compared with that of figure 3b for the 2D NS case. Figure 11 shows the instantaneous contour plots ("magnetic islands") for vector potential at $t = 117.19$.

In summary, the same qualitative behavior, with the role of the energy replaced by mean square vector potential, is seen for the 2D MHD case as was observed in the 2D NS case.

5. Algebraic Model

The indications are, for the runs reported in sections 3 and 4, that a steady state is being approached in which the fundamental dominates the spectrum, and the transfer to it is balanced by its own dissipation. This has led us to try a crude algebraic model of the dynamics of this process, which we illustrate for the 2D NS case.

Once the fundamental has begun to dominate, most of the new energy goes into the fundamental, so that $E \cong E(k_{min})$, $dE/dt \cong dE(k_{min})/dt$. We assume that the total enstrophy has become constant, $d\Omega/dt \cong 0$, and a significant fraction of the enstrophy may be lodged in the values of $k > k_{min}$ (as the Reynolds numbers increase, this conclusion should become more accurate). Let $\Omega = \Omega^1 + \Omega(k_{min})$, where $\Omega^1 = \sum_{k>k_{min}} \Omega(\underset{\sim}{k})$.

The evolution of the energy and enstrophy are now modelled by

$$\frac{dE}{dt} = -2\nu\Omega + f_E \tag{6}$$

$$\frac{d\Omega}{dt} = 0 = -2\nu \sum_{\underset{\sim}{k}} k^2\Omega(\underset{\sim}{k}) + k_F^2 f_E \tag{7}$$

where f_E is the rate of supply of energy by F and k_F is a wavenumber at the center of the forcing band.

f_E may be eliminated from equations (6) and (7) to give

$$\frac{dE}{dt} = -2\nu\Omega + \frac{2}{k_F^2} \Sigma_{\underset{\sim}{k}} k^2\Omega(\underset{\sim}{k})$$

or (noting that $k_{min}^2 = 1$),

$$\frac{dE}{dt} + 2\left(1 - \frac{1}{k_F^2}\right) E = -2\nu\Omega^1 + \frac{2\nu}{k_F^2} \sum_{k>k_{min}} k^2\Omega(\underset{\sim}{k}) \tag{8}$$

The right hand side of equation (8) can be evaluated in terms of the spectrum $|\underset{\sim}{v}(\underset{\sim}{k})|^2 = C_1 k^{-n_1}$ for k below the forcing band and $C_1 k^{-n_2}$ above it, with n_1, n_2, and C_1 taken from the computed values in figure 3b. The result is that equation (8) becomes of the form

$$\frac{dE}{dt} + \frac{1}{\tau} E = \frac{E_{max}}{\tau} \tag{9}$$

with $E_{max} \cong 3.58$ and $\tau \cong 254$ from the calculation. The solution, $E = E_{max}[1 - \exp(-t/\tau)]$ fits the shape of figure 1 rather well, but the numbers are not accurate, for $E_{max} \cong 3.9$ from figure 1, and $\tau = 124$. It might be, in the high Reynolds number limit, that this simple model in which the energy dissipation occurs mainly in the fundamental and balances the input, could be sharpened

considerably, but at such a low spatial resolution it has not seemed worthwhile to do so.

A similar development can be carried out for the 2D MHD case, with the resulting equation for A predicting $dA/dt = -A/\tau + A_{max}/\tau$, and a (comparably inaccurate) fit to the computed behavior can be obtained.

In summary, we believe that we have identified the correct qualitative behavior for the long-time state of the randomly forced 2D NS and 2D MHD equations in the presence of periodic boundary conditions. Namely, the fundamental continues to absorb the back-transferred quantity until it dominates the spectrum and may be limited only by its own dissipation.

Acknowledgments. This work was supported in part by the U.S. Department of Energy and in part by National Aeronautics and Space Administration Grant NSG-7416.

Appendix: Questions of Long-Term Accuracy

An obvious question which has no simple answer is whether there is a sense in which the code can be called accurate after the many eddy turnover times represented in these runs. Accuracy checks for such problems are few, and mostly consist of inferences drawn from conservation laws of the ideal invariants ("rugged" invariants) which survive the limitation to finite numbers of Fourier coefficients. The fact is that the code will not conserve these invariants out to the times we are reporting. These long times are dictated by the physics of the situation (it takes that long for the fundamental to come to dominate) and there are no totally conclusive statements about the accuracy that we can make.

We can, however, derive considerable reassurance from the following observations. Except for the very beginning ($t \lesssim 5$, say) there are no periods of time in which large qualitative changes occur in the behavior of the computed quantities. The code is accurate (in the above sense) over this initial time interval, and after that, there is only a slow, systematic evolution, always in the same direction. The code can be re-started and run accurately over any slice of time during the evolution after randomizing the phases of the Fourier coefficients: e.g., $\omega(\underset{\sim}{k}) \to \omega(\underset{\sim}{k}) \exp(i\phi)$ at some instant, where ϕ is a random number between $-\pi$ and π.

Figure 12 shows the results of such a typical restart at $t = 58.6$ for the 2D NS run, in a plot of $E(t)$ vs t. The two sets of random numbers F and G are the same sets of random numbers. There is no noticeable departure of the two solutions from each other, even after 10,000 time steps. Plotted in figure 13 are time averaged modal energy spectra for the two runs, over 1000 time steps ending at $t = 97.66$. Again, no noticeable differences appear.

The accumulation of round-off errors may appear as effectively only a slightly different set of random numbers provided by F and G.

If the problem is linearized and the amplification factor is calculated for the numerical scheme, an e-folding time turns out to be about $t = 2000$, whereas we have integrated only cut about $t = 275$.

These three considerations lead us to believe that what we have observed are properties of the randomly-forced 2D NS and 2D MHD equations, and not properties of the numerical scheme.

We believe the most serious limitation on the accuracy to be connected with the spatial resolution. Our computed Kolmogoroff dissipation wave number gets as large as 27 for the 2D NS case ($k_{max} = 16$) and as large as 33 for the 2D MHD case ($k_{max} = 16$). For this reason, we have run the additional segment of the 2D NS run as described in section 3. As noted there, no reversal of any of the observed properties was observed when the dissipation wavenumber was $\lesssim k_{max} = 32$.

References

BATCHELOR, G. K. 1969, Phys. Fluids 12, Suppl. II, 233.

BURG, J. P. 1975, Ph.D. Dissertation, Stanford University.

CARNEVALE, G. F., FRISCH, U., and SALMON, R. 1981, J. Phys. A: Math. and Gen. 14, 1701.

FJØRTOFT, R. 1953 Tellus 5, 225.

FRISCH, U., POUQUET, A., LÉORAT, J. and MAZURE, A. 1975, J. Fluid Mech. 68, 769.

FRISCH, U., POUQUET, A., SULEM. P.-L., and MENEGUZZI, M. 1983, J. de Mécanique Théorique et Appliquée [to appear].

FYFE, D. and MONTGOMERY, D. 1976, J. Plasma Phys. 16, 181.

FYFE, D., JOYCE, G., and MONTGOMERY, D., 1977a, J. Plasma Phys. 17, 317.

FYFE, D., JOYCE, G., and MONTGOMERY, D., 1977b, J. Plasma Phys. 17, 369.

GOTTLIEB, D. and ORSZAG, S. A. 1977, Numerical Analysis of Spectral Methods: Theory and Applications [Philadelphia: Society for Industrial and Applied Mathematics].

KRAICHNAN, R. H., 1967 Phys. Fluids 10, 1417.

KRAICHNAN, R. H. and MONTGOMERY, D. 1980 Rept. Prog. Phys. 43, 547.

LEITH, C. E. 1968 Phys. Fluids 11, 571.

LILLY, D. K. 1969, Phys. Fluids 12, Suppl. II, 240.

MATTHAEUS, W. H. 1982, Geophys. Res. Lett. 9 (6), 660.

MATTHAEUS, W. H. and MONTGOMERY, D. 1980, Ann. N.Y. Acad. Sci. 357, 203 [Proc. Intl. Conf. on Nonlinear Dynamics].

MATTHAEUS, W. H. and MONTGOMERY, D. 1981, J. Plasma Phys. 25, 11.

MENEGUZZI, M., FRISCH, U., and POUQUET, A., 1981, Phys. Rev. Lett. 47, 1060.

MONTGOMERY, D. 1975, in Plasma Physics: Les Houches 1972, ed. by C. de Witt and J. Peyraud, pp. 427-535 (New York, Gordon & Breach).

ONSAGER, L. 1949, Nuovo Cimento Suppl. 6, 279.

ORSZAG, S. A. 1971, Stud. Appl. Math 50, 293.

ORSZAG, S. A. and TANG, C.-M., 1979, J. Fluid Mech. 90, 129.

PATTERSON, G. S. and ORSZAG, S. A., 1971, Phys. Fluids 14, 2538.

POUQUET, A., 1978 J. Fluid Mech. 88, 1.

POUQUET, A., FRISCH, U., and LÉORAT, J. 1976 J. Fluid Mech. 77, 321.

Figure Captions

Figure 1. Total energy vs. time for forced 2D NS run. Squares are the contributions of the fundamental, $k^2 = k^2_{min} = 1$.

Figure 2. Total enstrophy vs. time for same 2D NS run shown in figure 1.

Figure 3a. 2D NS modal energy spectrum, averaged over all $\underset{\sim}{k}$ for given k^2, vs. k^2. Averages are taken over 1000 time steps ending at t = 29.30. Forcing band is $55 \leq k^2 \leq 70$.

Figure 3b. Same as figure 3a, except time averages are over 1000 time steps ending at t = 273.44. Note dominance of the fundamental, $k^2 = 1$.

Figure 4. Contours (streamlines) ψ = const. for 2D NS run at t = 273.44.

Figure 5. Temporal history of a typical ($\underset{\sim}{k}$) modal energy for 2D NS run. Value shown has $|\underset{\sim}{k}|^2 = 50$.

Figure 6. Carnevale entropy vs. time for 2D NS run.

Figure 7. Total mean square vector potential vs. time for forced 2D MHD run. Squares are contributions of fundamental $k^2 = 1$. Run goes from $(32)^2$ to $(64)^2$ at t = 97.66.

Figure 8. Total energy vs. time for 2D MHD forced run shown in figure 7. "B" = magnetic energy; "V" = kinetic energy.

Figure 9. Spectrum $|A(\underset{\sim}{k})|^2 = |B(\underset{\sim}{k})|^2/k$ for mean square vector potential for 2D MHD run shown in figures 7 and 8. Average is over all $\underset{\sim}{k}$'s corresponding to same k^2 and over 50 values 100 time steps apart ending at t = 97.66.

Figure 10. Spectrum $|A(\underset{\sim}{k})|^2 = |B(\underset{\sim}{k})|^2/k^2$ for forced 2D MHD run at $(64)^2$, averaged over 25 values 100 time steps apart, ending at t = 117.19. Note the dominance of the fundamental $k^2 = 1$.

Figure 11. Contours of constant a (field lines) at t = 117.19 for forced 2D MHD run.

Figure 12. The result of randomization of phases of a 2D NS run. Two runs are identical up to t = 58.6 (arrow). Then the phases are randomized for one run and the two become distinct beyond that time. The departures of the circles from the crosses indicate the divergence of the two runs thereafter.

Figure 13. Modal energy spectra for the two runs shown in figure 12. Note that the fundamental ($k^2 = 1$) values are essentially identical.

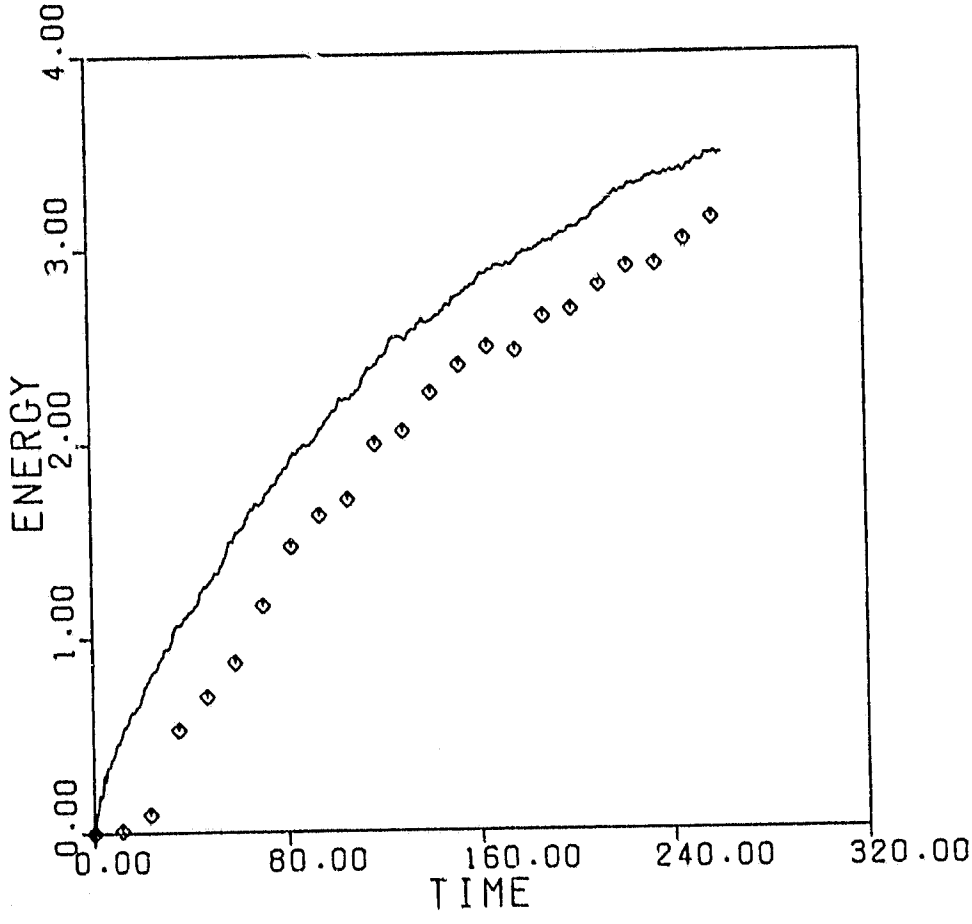

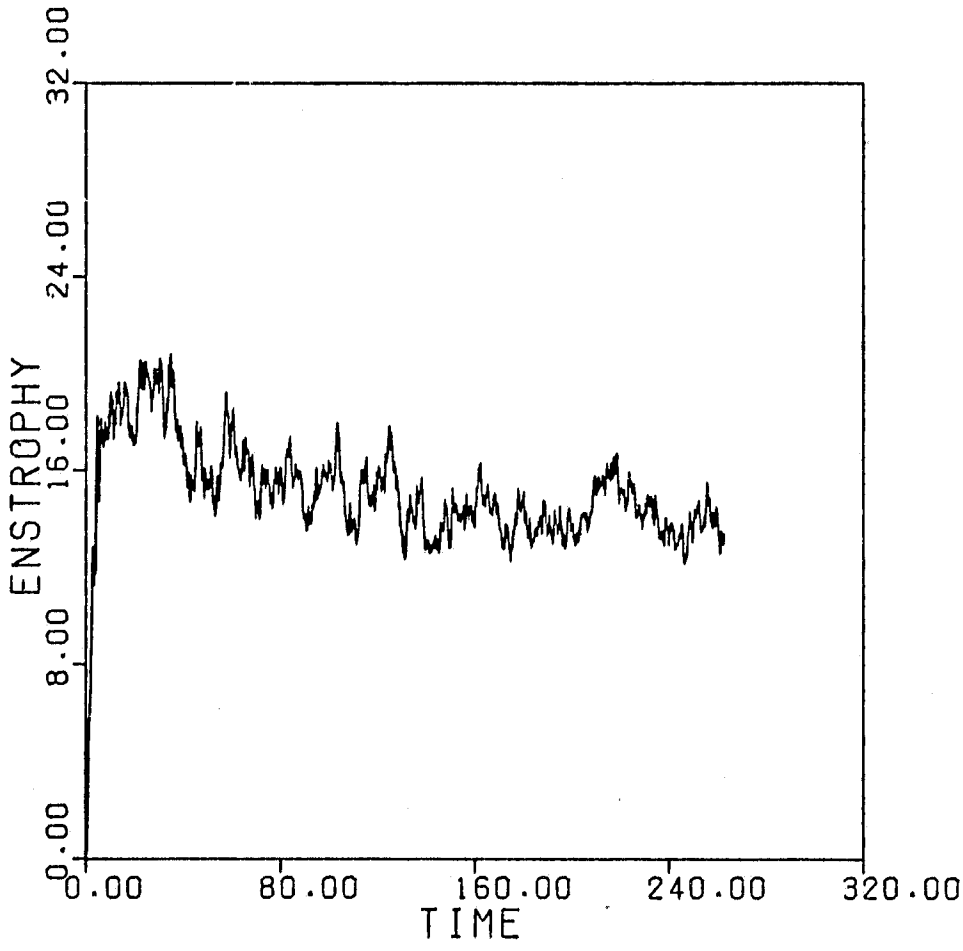

AVERAGED OVER 1000 TIME STEPS
ENDED AT T= 29.30
TIME STEPS 6501 TO 7500

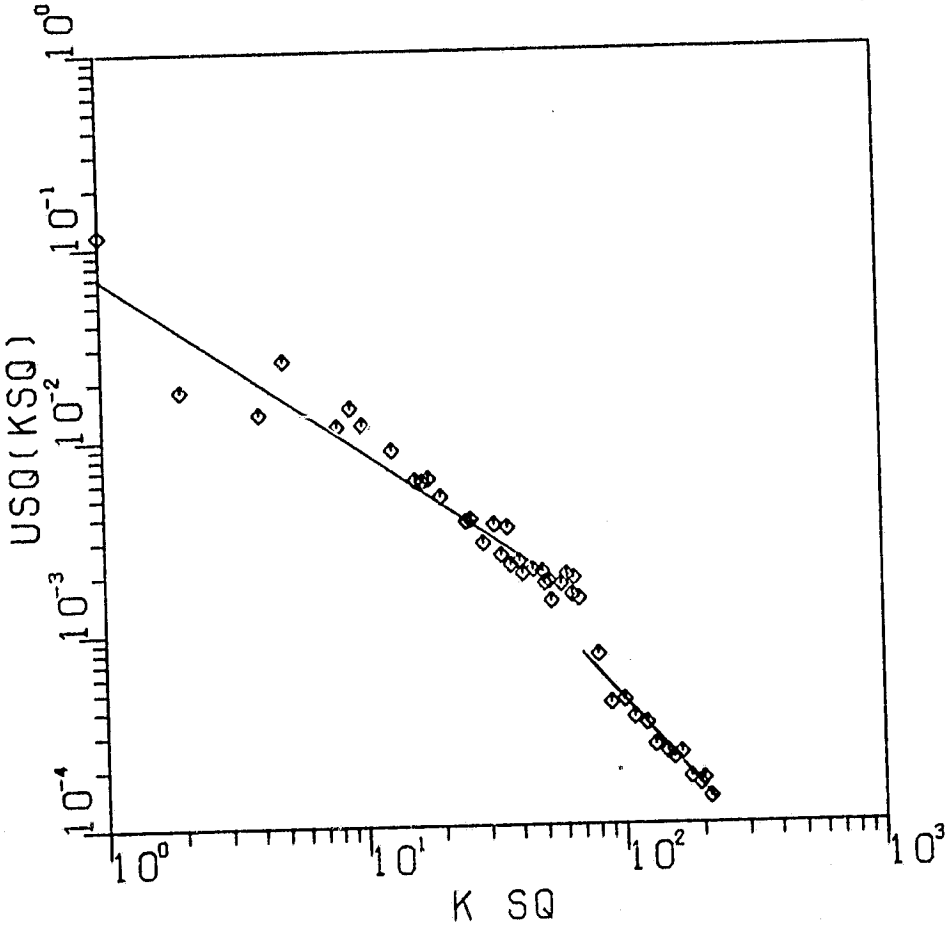

AVERAGED OVER 1000 TIME STEPS
ENDED AT T= 273.44
TIME STEPS 69000 TO 69999

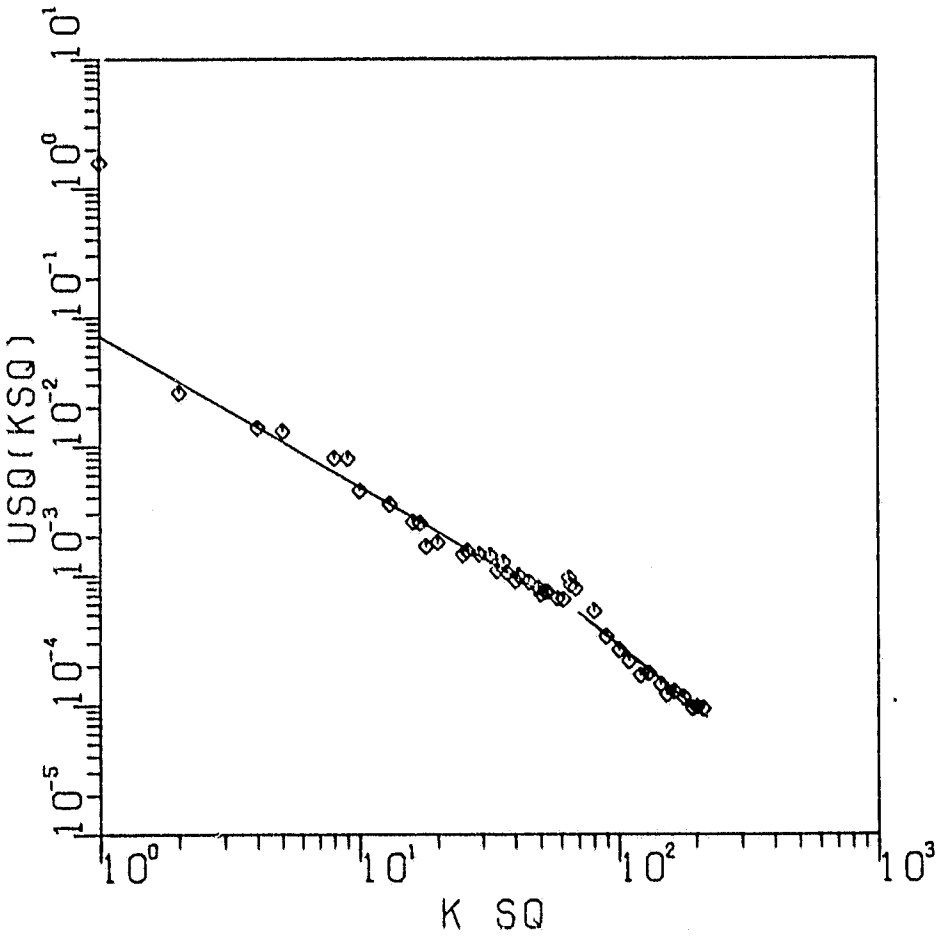

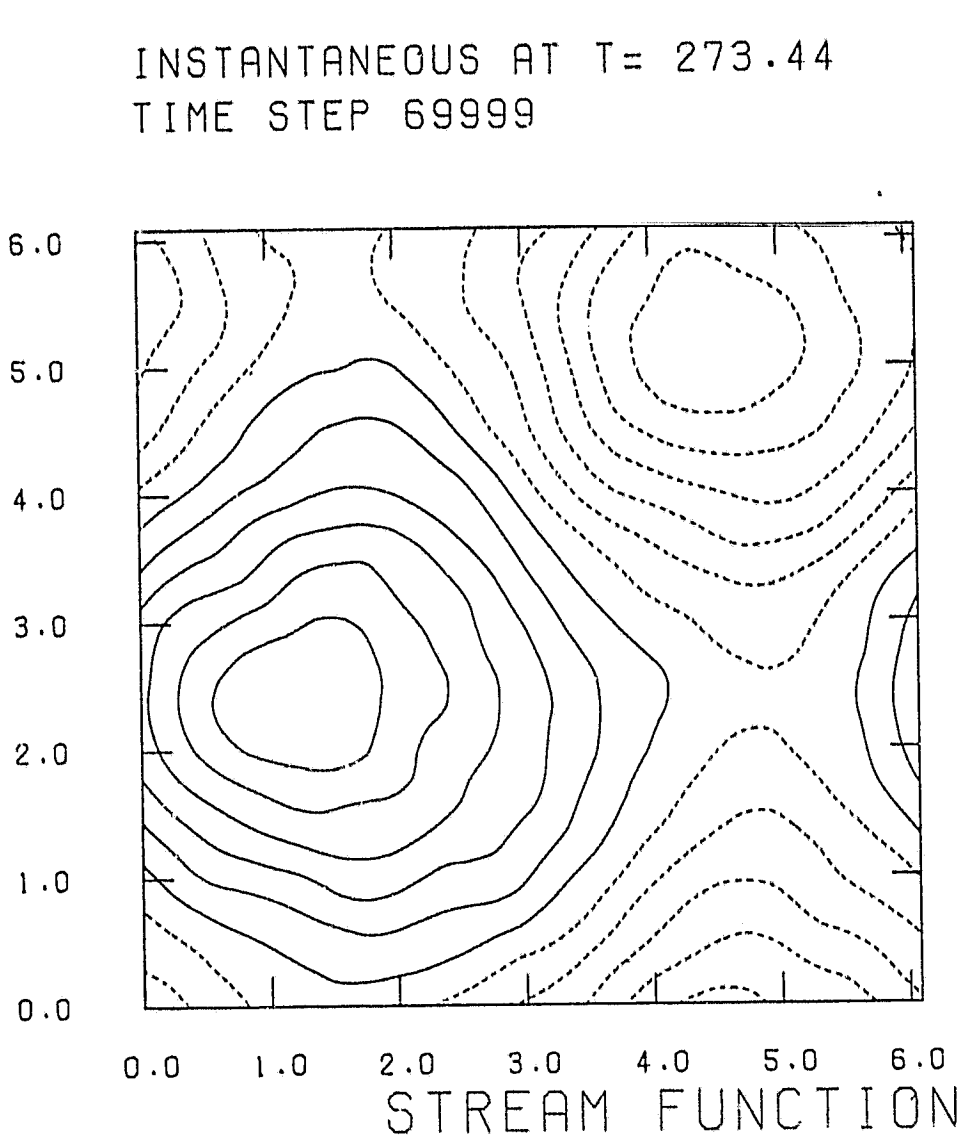

KSQ= 50

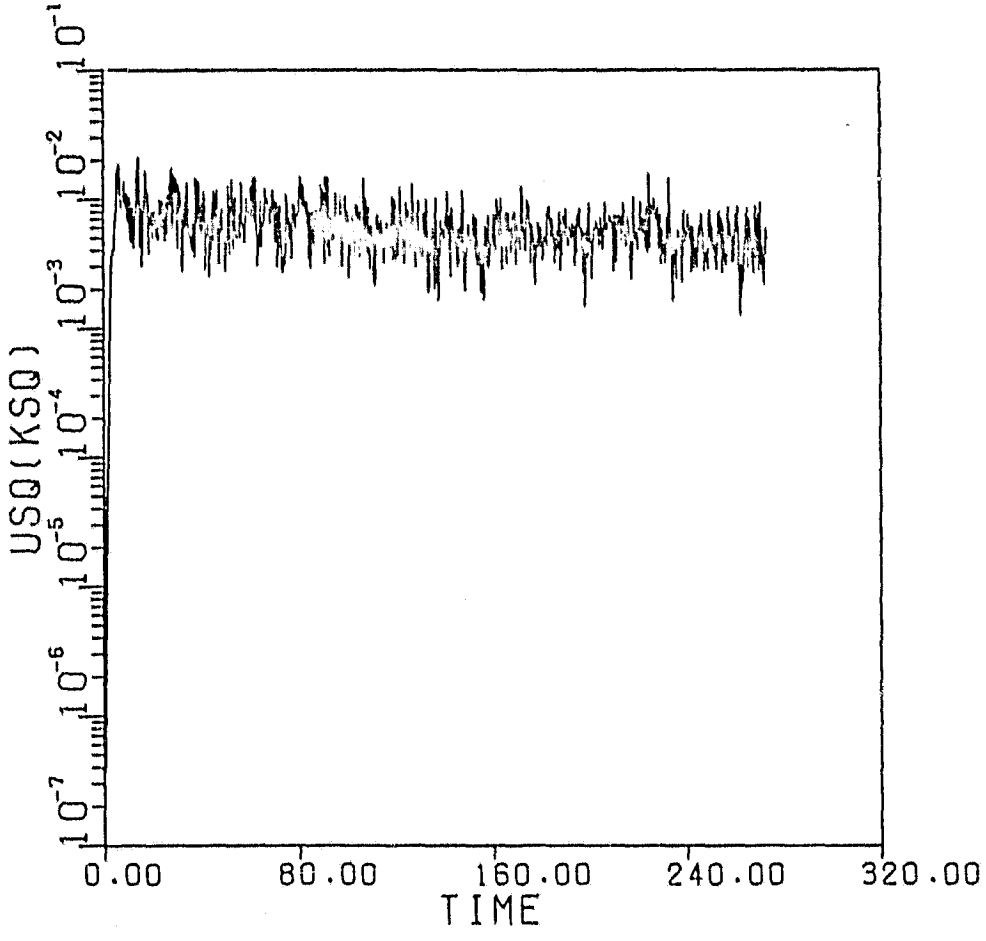

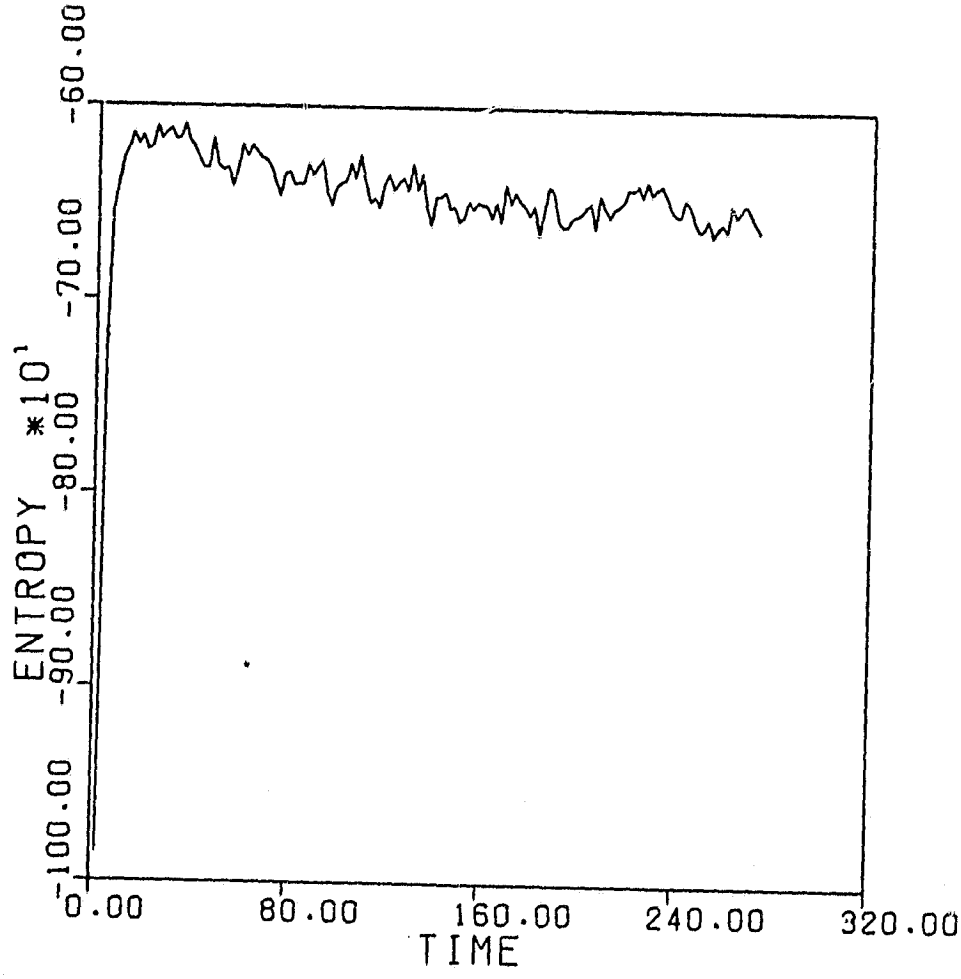

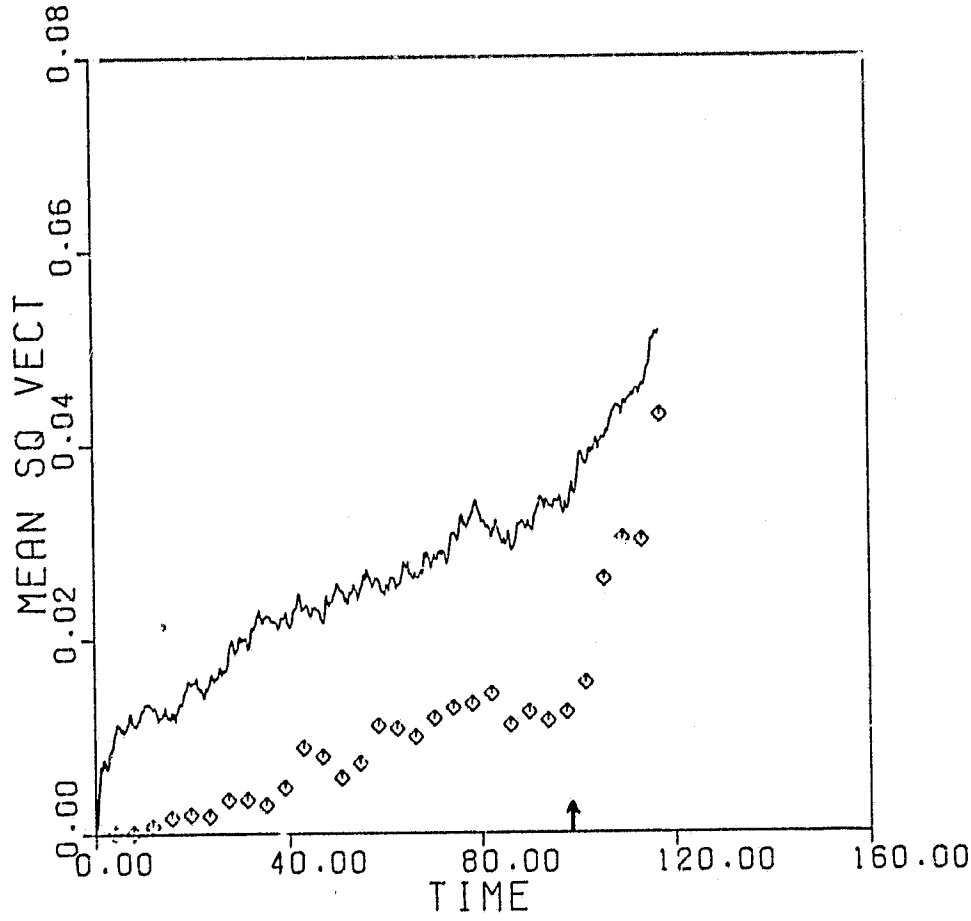

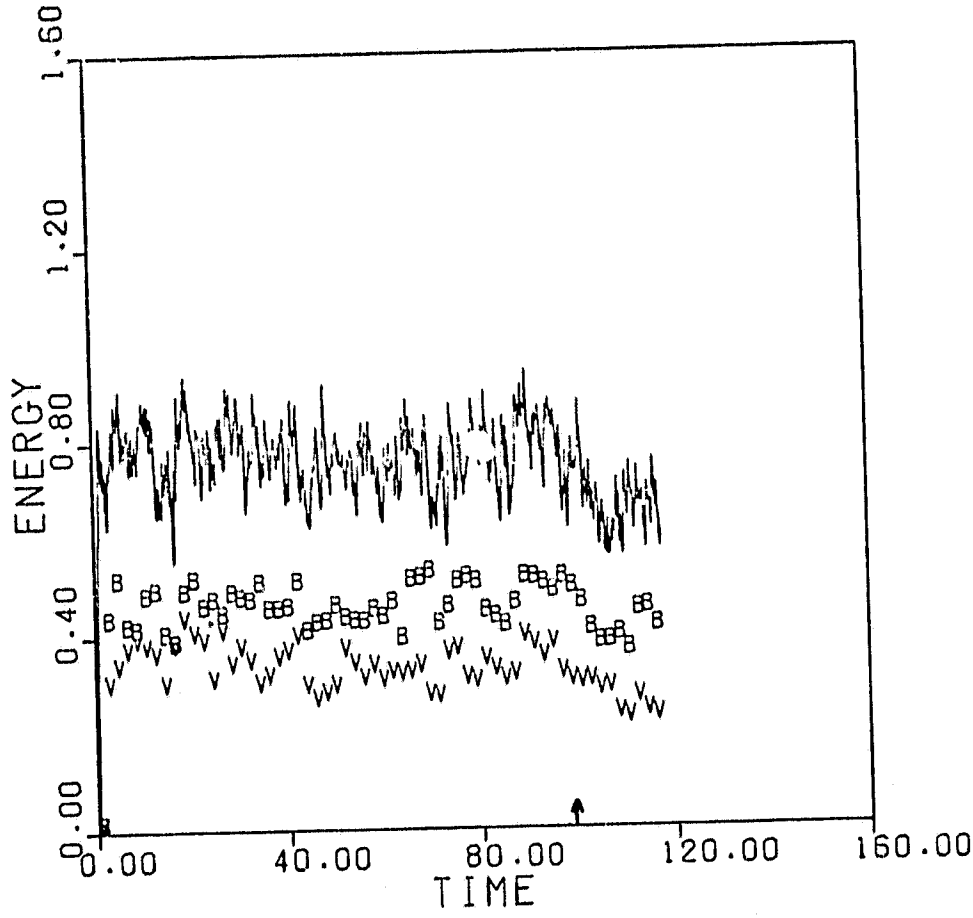

ASQ(KSQ)

AVERAGED OVER 50 SNAP SHOTS
ENDED AT T= 97.66

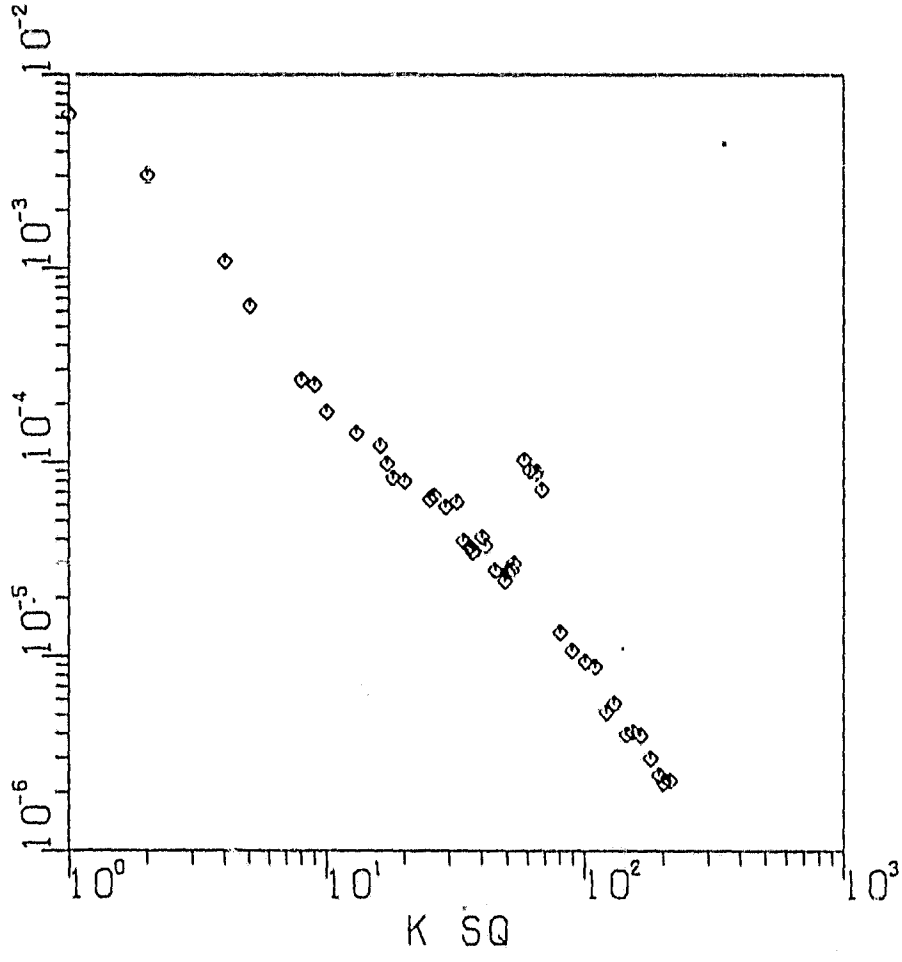

ASQ(KSQ)

AVERAGED OVER 25 SNAP SHOTS
ENDED AT T= 117.19

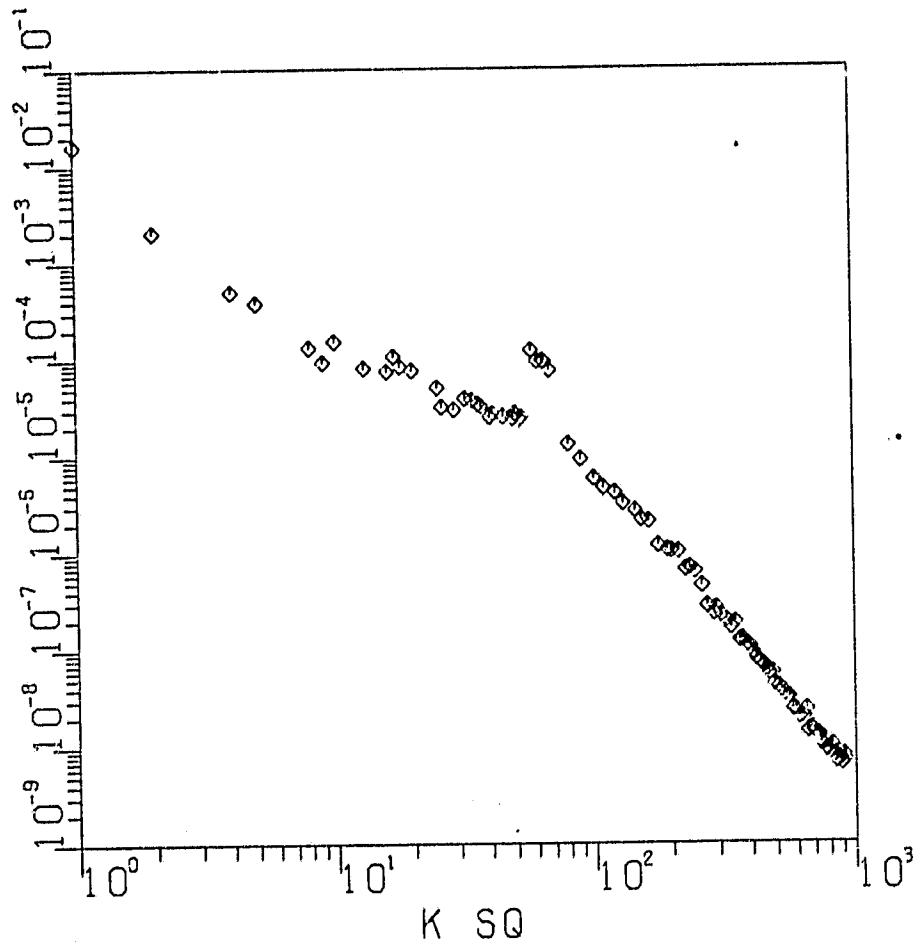

INSTANTANEOUS AT T= 117.19
TIME STEP 30000

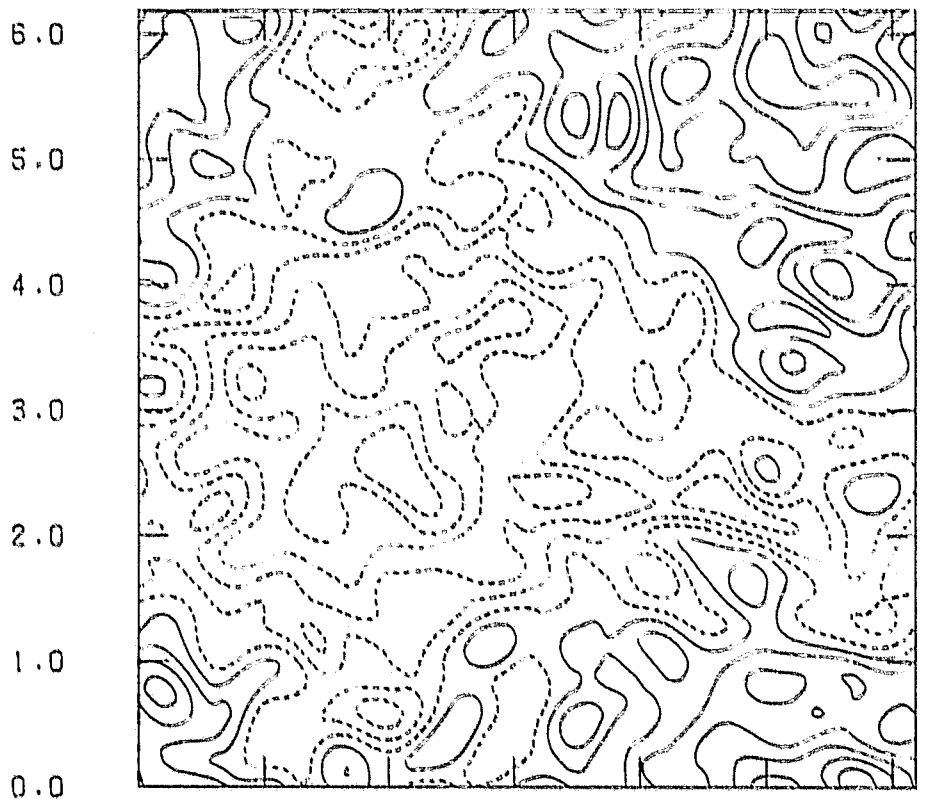

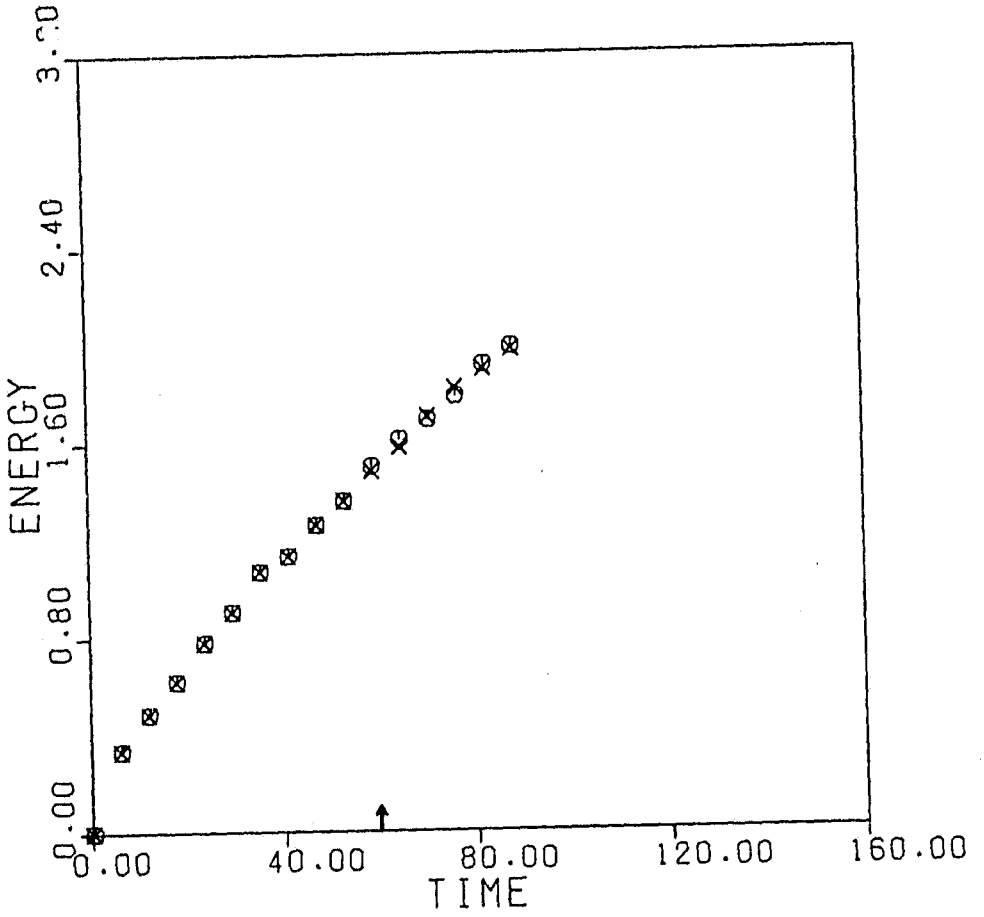

AVERAGED OVER 1000 TIME STEPS
ENDED AT T= 97.66
TIME STEPS 24001 TO 25000